THE UNIVERSALITY OF NBTI RELAXATION AND ITS IMPLICATIONS FOR MODELING AND CHARACTERIZATION

Tibor Grasser*, Wolfgang Gös*, Victor Sverdlov†, and Ben Kaczer°
* Christian Doppler Laboratory for TCAD at the †Institute for Microelectronics, Gußhausstraße 27–29, A-1040 Wien, Austria
° IMEC, Kapeldreef 75, B-3001 Leuven, Belgium

ABSTRACT

As of date many NBTI models have been published which aim to successfully capture the essential physics [1–5]. As such, these models have mostly focused on the stress phase. The relaxation phase, on the other hand, has not received as much attention, possibly because of the contradictory results published so far. Particularly noteworthy are the very long relaxation tails of almost logarithmic nature [5–7], which cannot be successfully described by the reaction-diffusion model [7]. We argue that understanding the nature of the relaxation phase could hold the key to unraveling the underlying NBTI mechanism. In particular, we stipulate that the relaxation phase follows a universal relaxation 'law' [6, 8–10], demonstrate the valuable consequences resulting therefrom, and use this universality to classify presently available NBTI models.

I. INTRODUCTION

Although being known for forty years [11], negative bias temperature instability (NBTI) is attracting an ever growing industrial and scientific attention as one of the most important reliability issues in modern CMOS technology. NBTI is mostly described by a shift of the threshold voltage when a typically large negative voltage is applied to the gate of a pMOS at elevated temperatures [12, 13]. In the following we assume that during NBT stress the change in the density of interface states, which are commonly assumed to be P_b centers [14], is given through $\Delta N_{it}(t)$. It is assumed that charging and discharging of these interface states is very fast, and consequently that the positive charge in these interface states follows the Fermi-level via

$$\Delta Q_{it}(t) = q \int \Delta D_{it}(E_t,t)\, f(E_F,E_t,t)\, dE_t \ . \qquad (1)$$

Here, ΔD_{it} is the time-dependent density of interface states, which is by a still to be quantified relation directly linked to $\Delta N_{it}(t)$ [15], and $f(E_t)$ their occupancy. During NBT stress, the Fermi-level E_F is close to the valence band edge and $f(E_t) \approx 1$ throughout the silicon bandgap. Thus, during stress, under the assumption that P_b-centers introduce states only *within* the silicon bandgap, see [4] for a different interpretation, all newly generated interface states ΔN_{it} are positively charged and one obtains independently of the exact form of the density-of-states $\Delta Q_{it}(t) \approx q\Delta N_{it}(t)$. This is the usual assumption employed for instance in the reaction-diffusion model.

On top of generated interface defects, charge may be stored in existing or newly created oxide traps. Although most of these traps may still be considered 'fast', they are more difficult to charge and discharge, that is, have larger time constants than interface states due to their location inside the oxide bulk. Thus, their occupancy cannot follow the Fermi-level and $\Delta Q_{ox}(t)$ will be governed by different dynamics. The contribution of the oxide charges to the threshold voltage shift is formally written as

$$\Delta Q_{ox}(t) = q \iint \Delta D_{ox}(x,E_t,t)\, f_{ox}(x,E_t,t)\, (1 - x/t_{ox})\, dx\, dE_t \ , \qquad (2)$$

with ΔD_{ox} being the spatially and energy-dependent density-of-states in the oxide, f_{ox} the occupancy of these traps, and t_{ox} the oxide thickness. Note that the issue of whether oxide charges are important during NBTI or not is one of the most controversial at the time [2, 4, 16, 17]. Also, the question whether ΔD_{ox} consists mainly of pre-existing traps [2, 16] or traps that are created during stress [4] remains to be answered.

Other potential contributions to a threshold voltage shift like mobile charges are commonly assumed to be negligible in the context of NBTI and the total threshold voltage shift is thus given by

$$\Delta V_{th}(t) = \frac{\Delta Q_{it}(t) + \Delta Q_{ox}(t)}{C_{ox}} \ . \qquad (3)$$

During stress, most measurements indicate that $\Delta V_{th}(t)$ follows a power-law as At^n [12]. However, log-like behavior, in particular at short times, has also been reported [7, 18, 19].

The fundamental problem in the context of NBTI is given by the fact that the damage created during the stress phase begins to recover immediately once the stress is removed. This makes the classic measurement technique where the stress is interrupted during the extraction of the threshold voltage problematic [7, 20]. In particular, the value of the extracted power-law exponent depends significantly on the delay introduced during the measurement [5, 17, 21]. Experimental results obtained with delayed measurements show a linear increase of the exponent with temperature [5, 17, 22] with values around $0.2 - 0.3$. In contrast, temperature-independent exponents in the range $0.07 - 0.2$ have been extracted from recent delay-free measurements [9, 19, 23]. Of particular interest is the question related to the origin of this relaxation. While some authors assume that hole trapping is negligible and both degradation as well as relaxation is determined by the temporal change of the interface state density [17], others acknowledge at least partial importance of trapped charges [4, 19, 22, 24]. In the latter case it has been assumed that trapped charges either form the 'fast' component of NBTI relaxation superimposed onto some interface defect relaxation [19, 24] or are solely responsible for any recovery while created interface defects do not recover at all [4, 22].

II. MEASUREMENT ISSUES

The understanding and characterization of NBTI is considerably hampered by the difficulties arising during measurement. Currently, two techniques are used to characterize NBTI: the classic measurement/stress/measurement (MSM) technique, which is handicapped by undesired relaxation, and on-the-fly (OTF) measurements which avoid any relaxation by maintaining a high stress level throughout the measurement and directly monitor the drain current in the linear regime, $\Delta I_{D,lin}$. Since it is the threshold voltage shift ΔV_{th} rather than $\Delta I_{D,lin}$ that is relevant for design purposes, $\Delta I_{D,lin}$ has to be converted into the more relevant ΔV_{th} which involves some approximate relations [22] or an empirical formalism [25]. This issue is of particular importance during the assessment of the relaxation phase: When V_G is

1-4244-0918-7/07/$25.00 ©2007 IEEE

IEEE 07CH37867 45th Annual International Reliability Physics Symposium, Phoenix, 2007

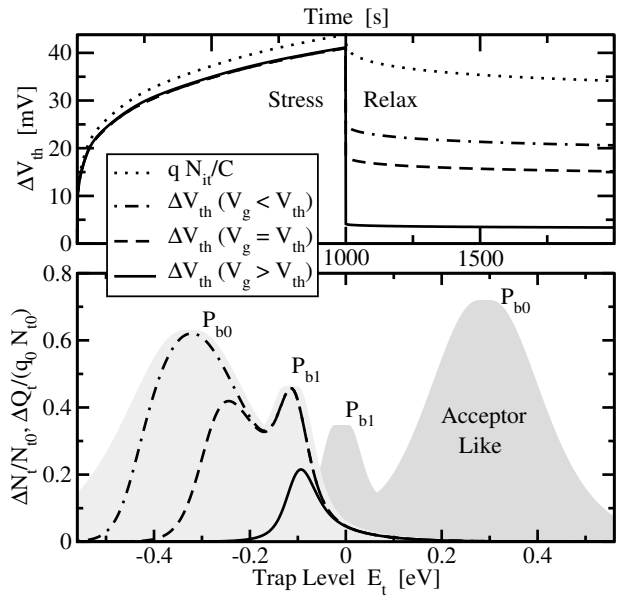

Fig. 1: Influence of the interface state occupancy on the observed threshold voltage shift during OTF measurements. During stress, nearly all interface traps are positively charged. When a different gate voltage is used during relaxation, only a fraction of the traps are visible which must be separated from the real relaxation. Schematically shown is the density-of-states typically associated with P_{b0} and P_{b1} centers [26].

left at V_G^{relax} [6], the interface trap occupancy is considerably lower than during the stress phase [15], resulting in spurious additional relaxation (Fig. 1). Conversely, when V_G is brought back to V_G^{stress} [9], one faces the opposite problem one is trying to avoid during the stress phase, since now additional uncontrolled stress is introduced during the measurement cycles. Even more important is the fact that the initial value of $I_{D,lin}$ is extremely difficult to determine as it is already obtained at the stress voltage. Conventionally, the time required for this is in the milliseconds range where already significant degradation can be observed [19] but any uncertainty in $I_{D,lin}$ modifies the time exponent (the 'slope') of ΔV_{th} on a log-log plot. This may render many results obtained by the OTF technique questionable. In contrast, the MSM technique probes the interface under comparable conditions during both the stress and relaxation phase. In addition, the voltage applied to the gate is close to the threshold-voltage where only negligible degradation can be expected. However, as is shown below, it is probably **very difficult to minimize the measurement delay** in such a way that the true degradation is observed.

III. Characterization of Relaxation

To formally distinguish between the degradation during the stress and relaxation phases we use the term $S(t_s)$ for the real damage accumulated during the stress phase. As soon as the stress voltage is removed, relaxation sets in as a function of the accumulated stress time t_s and the relaxation time $t_r = t - t_s$, which will be denoted as $R(t_s,t_r)$. Furthermore, we introduce $S_M(t_s,t_M)$ as the observed damage during an MSM sequence with a measurement delay of t_M.

Since the damage $S(t_s)$ is known to relax as soon as the stress voltage is removed, possible at timescales shorter than a microsecond [7], a rigorous characterization of the relaxation phase is extremely challenging. Typically, the relaxation data $R(t_s,t_r)$ recorded at different stress times t_s have been normalized to the first measurement point t_M as $r_f(t_s,t_r) = R(t_s,t_r)/R(t_s,t_M)$, the *fractional recovery*, and aligned

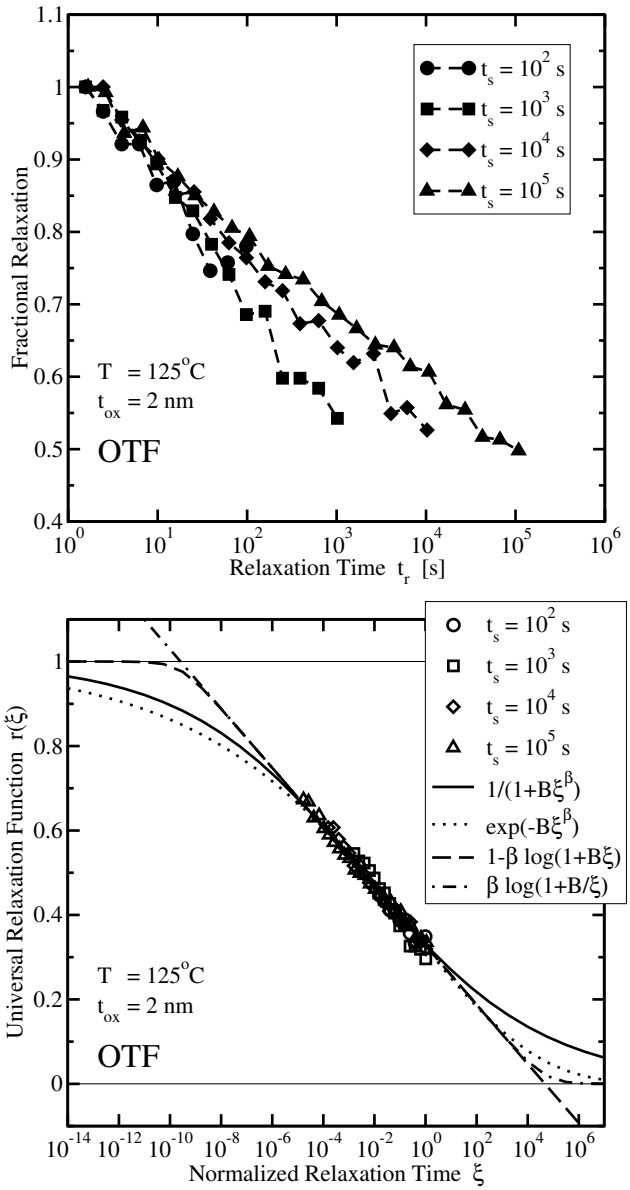

Fig. 2: Demonstration of universal recovery for the OTF data of Denais *et al.* [10]. The top figure shows a conventional view of the fractional recovery as a function of the relaxation time t_r. Apparently, data obtained after longer stress times, seems to relax more slowly than data obtained at shorter times. The bottom figure, on the other hand, demonstrates the universality of relaxation when the relaxation data is normalized to the last stress value and plotted over the ratio $\xi = t_r/t_s$ [10]. Also shown are some possible empirical expressions which can be fit to the data.

as a function of the absolute relaxation time t_r [5–8], see Fig. 2. Although the functional form of the relaxation remains illusive in such a plot, Rangan *et al.* [8] were the first to observe certain features of a universality in the relaxation. This and subsequent studies can be summarized as follows:

R1) Recovery does not level off even at the shortest times [8] which implies that it is difficult to asses the real damage a $t_r = 0$. This is even true for the ultra-fast data obtained by Reisinger *et al.* [7] with $t_M = 2.2\,\mu$s.

R2) For longer stress times, the relaxation apparently slows down [5,

8, 9], that is, the fractional recovery becomes smaller, as visible in Fig. 2.

R3) Independent of the stress field, the fractional recovery is roughly similar [8].

R4) The universality as proposed by Rangan *et al.* has been studied by Krishnan *et al.* [9], who observed that the fractional recovery is even independent of the stress-time. This, as also pointed out by Krishnan *et al.*, is somewhat in disagreement with R2 which states that the fractional recovery becomes smaller with larger stress times.

R5) Recovery seems to reset a certain fraction of the defects to their original state, as proven by re-stress experiments [8, 22].

R6) Denais *et al.* [10] realized that the relative recovery obtained after different stress times follows the same pattern when plotted as a function of relaxation time over stress time, $\xi = t_r/t_s$, see Fig. 2.

R7) Contradicting evidence is available regarding the recovery field-dependence, where [8, 17] report no field-dependence contrary to [5, 22] who observe a strong field-dependence.

As will be shown, the universality described by Denais *et al.* is both the most intriguing and consequential feature as it has a fundamental impact on any theoretical understanding of NBTI and should therefore be an important ingredient in any modeling attempt. Considering also the fact that not all damage can recover, that is, that there could be a permanent component $P(t_s)$ [8, 27], we rewrite the accumulated damage as $S(t_s) = R(t_s,0) + P(t_s)$ and introduce the universal relaxation function as

$$r(\xi) = \frac{R(t_s,t_r)}{S(t_s) - P(t_s)} = \frac{R(t_s,t_r)}{R(t_s,0)} \tag{4}$$

and discuss its properties and consequences in the following. Note the relation between the universal recovery function and the fractional recovery given by $r_f(t_s,t_r) = r(\xi)/r(\xi_M)$ with $\xi_M = t_M/t_s$. Since the data available to us does not definitely support the existence of a permanent component, we will assume the permanent component to be negligible in the following and assume $P(t_s) = 0$.

A. Functional Form of the Relaxation

Lacking a universally accepted and valid theory for NBTI, the exact form of the universal relaxation function $r(\xi)$ remains illusive at this point and we will have to empirically estimate $r(\xi)$ in the following. Various empirical expressions have already been suggested and fit to measured relaxation data. Generalized for universality, these expressions include $r(\xi) = 1 - B\xi^\beta$ [28], $r(\xi) = 1 - B\log(\xi)$ [29], and $r(\xi) = 1 - C(1 - \exp(-B\xi))$ [30]. These expressions are problematic as they either have no asymptotic limit for large and/or small ξ, or they do not capture recent measurement data. In particular, we will show that the limit $r(\xi \to 0)$ is of considerable practical value and should be meaningful in any analytic expression.

Interestingly, NBTI models operating in the diffusion-limited regime, be it classic [29] or dispersive diffusion [5], agree that the relaxation depends on the ratio $\xi = t_r/t_s$ only, that is, they are universal in our sense. For the reaction-diffusion (RD) model Alam [29] derived the approximate solution $r(\xi) = 1 - \sqrt{\gamma\xi/(1+\xi)}$ with the empirical parameter $\gamma \approx 0.5$. Although this expression is accurate for small ξ, for large ξ it has the limit $1 - \sqrt{\gamma}$ which for $\gamma \neq 1$ does not agree with the numerical solution of the RD model which exactly goes to zero. It can be shown that the power-law-like expression

$$r(\xi) = 1/(1 + \xi^{1/2}) \tag{5}$$

agrees very well with the numerical solution over the whole range of relaxation times (cf. Fig. 12). Generalizing the RD model to allow for dispersive transport of the hydrogen-species, Kaczer *et al.* [5] derived

$$r(\xi) = 1/(1 + \xi^{\alpha/2}) \tag{6}$$

with α being the dispersion parameter ($\alpha \in [0 \ldots 1]$). Note that in the diffusive limit where $\alpha = 1$, the RD result is retained. However, as will become clear in the sequel, neither (5) nor (6) can cover the whole range of available measurement data and we will use the generalized form

$$r(\xi) = 1/(1 + B\xi^\beta) \tag{7}$$

where the parameters B and β are in the range $B \approx 0.3 - 3$ and $\beta \approx 0.15 - 0.2$ for most of the data available to us.

Since the exact form of the relaxation function has important implications on the interpretation of the measurement data, we also consider alternative expressions. First, we note that relaxation in disordered systems has long been described using a stretched-exponential [31]

$$r(\xi) = \exp(-B\xi^\beta) \ . \tag{8}$$

Also, Denais *et al.* [10] suggested the empirical expression

$$r(\xi) = 1 - \beta\log(1 + B\xi) \ , \tag{9}$$

while Huard *et al.* [18] used the analytic solution of a hole-trapping problem derived in [32] which appears to be of a similar form (see Section VII-C for a discussion)

$$r(\xi) = \beta\log(1 + B/\xi) \ . \tag{10}$$

We note that (9) has no useful limit for large ξ while (10) goes to infinity for $\xi \to 0$. Since we will make extensive use of the latter limit, we will use the empirical relation (9) in our comparisons, noting that the singularity in the physics-based expression (10) is a consequence of the simplifications employed in the derivation presented in [32] and does of course not exist in the full numerical solution. Nevertheless, both expressions are equivalent for intermediate values of ξ and will be labeled 'log-like' in the following.

The expressions summarized above are compared in Fig. 2. All expressions can be fit to the measurement data and give fits of practically the same accuracy. However, they result in different extrapolations for large and small relaxation times, the consequences of which need to be carefully studied.

IV. Characterization of MSM Data

Although more delicate to apply, universal relaxation is of particular interest for data obtained by the MSM technique. For the normalization needed in (4) one has to keep in mind that the value of $S(t_s) = R(t_s,0)$ is essentially unknown, one only knows $R(t_s,t_M)$ determined at the first measurement point available after a short relaxation period t_M. However, making use of the universal relaxation expression (4) and *assuming* for the time being that $r(\xi)$ is known, $S(t_s) = R(t_s,0)$ can be obtained as

$$S(t_s) = \frac{R(t_s,t_M)}{r(t_M/t_s)} \ . \tag{11}$$

Inserting the above into the universal relaxation relation (4) we obtain

$$\frac{r(\xi)}{r(\xi_M)} = \frac{R(t_s,t_r)}{R(t_s,t_M)} \ . \tag{12}$$

From (12) the as of yet unknown parameters B and β can be easily determined from a measured sequence of relaxation points $R(t_s,t_r)$,

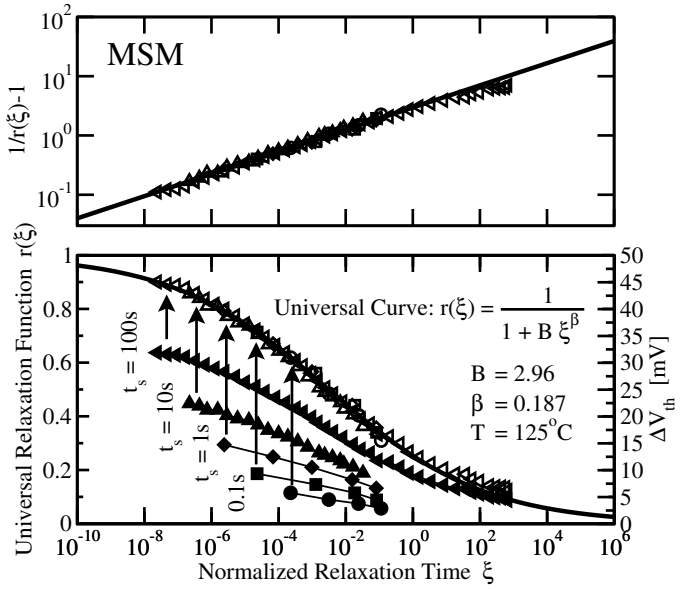

Fig. 3: Application of universal relaxation to the ultra-fast MSM data obtained by Reisinger *et al.* [7]. Depending on the choice of the universal relaxation function, the individual data points can be mapped onto the respective universal curve, in this case (7). Note the linear behavior of $1/r-1$ shown in the upper plot. The slight deviation for $\xi > 10^2$ could bear the hint of a permanent component $P(t_s)$.

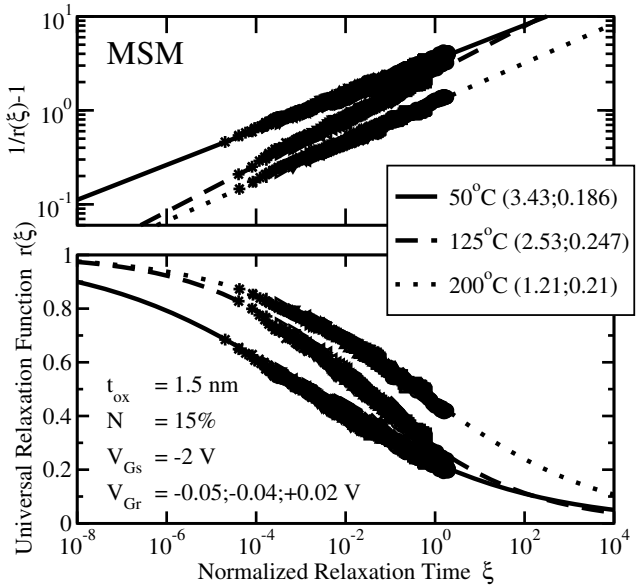

Fig. 4: Same as Fig. 3 but with data from IMEC [5]. Relaxation data of three devices stressed in a single MSM sequence were recorded at 10 different stress-times in the interval $10\,\mathrm{s} - 10^4\,\mathrm{s}$ at three different temperatures. The values of B and β (given in parenthesis) depend on the temperature, β even in a non-monotonic manner which might indicate the existence of two different processes with different temperature dependencies [7].

see for example Fig. 3. Naturally, in contrast to data obtained by OTF measurements where $R(t_s,0)$ is known, the analytical expression determines the final value of $R(t_s,0)$ through the extrapolation given by (12). This results in a 'floating' behavior of $r(\xi_M)$ which reflects the uncertainty of this approach.

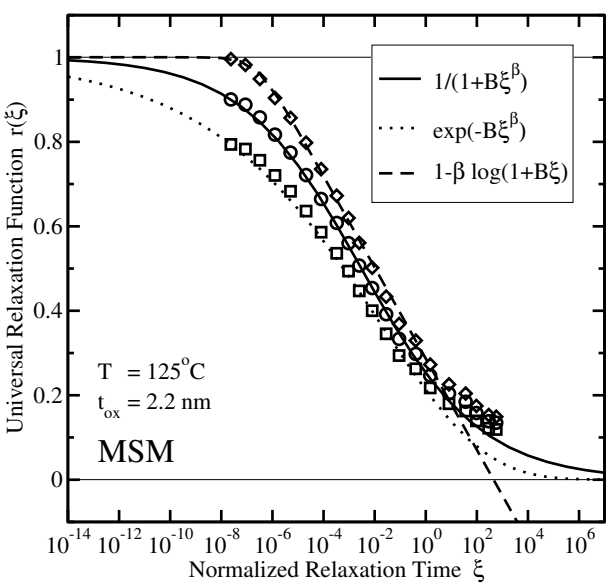

Fig. 5: The uncertainty introduced by extrapolating back to $t_M = 0$ using a particular relaxation function. This uncertainty is in the order of 10% for the relaxation functions considered here. For the sake of clarity, only the $t_s = 100\,\mathrm{s}$ data of Reisinger *et al.* [7] is shown. Note that the different extrapolations to $t_M = 0$ shift the same measurement data (various symbols) by a multiplicative factor.

Before looking at this issue, however, we consider the case of a typical MSM sequence. We recall that during MSM sequences the duration of the stress intervals usually grows exponentially while the measurement interval t_M is short and of constant duration. This implies that after a certain stress time, which we determined empirically to be of the order $t_s \gtrsim 10 \times t_M$, the relaxation during the measurement does not significantly alter the damage at the *end* of each stress phase, meaning that the damage relaxed during each measurement interval is mostly restored during the next stress phase. Consequently, equation (11) holds for every stress point t_s, where t_s is now the accumulated net stress time. For the particular case of the RD model we will show later that this is an excellent approximation. The likely correctness of this assumption for real measurement data is demonstrated in the following. First, the application of the above procedure to the detailed relaxation data published by Reisinger *et al.* [7] is studied in Fig. 3 and for the IMEC data otherwise published in [5] in Fig. 4, where the universality is shown at three different temperatures, 50 °C, 125 °C, and 200 °C.

A. Uncertainty Related to the Analytic Expression for $r(\xi)$

In Fig. 3 and Fig. 4, the universality has been demonstrated using the relaxation expression (7). Naturally, one may inquire about the influence of the universal relaxation function on the final result. This issue is explored in Fig. 5, where the above procedure is performed using the universal relaxation functions (7), (8), and (9). Although all expressions considered here can be fit to the measurement data, the different predictions for the extrapolated value at $t_M \to 0$ result in an uncertainty of roughly 10%. Unfortunately, the data available to us at the moment is not conclusive to decide on the best approximation for r, but the power-law-like expression (7) gives the best fit over the entire range also including large relaxation times, while the log-like expression might slightly better capture the saturation for small times. The slight deviation for $\xi > 10^2$ could bear the hint of a permanent

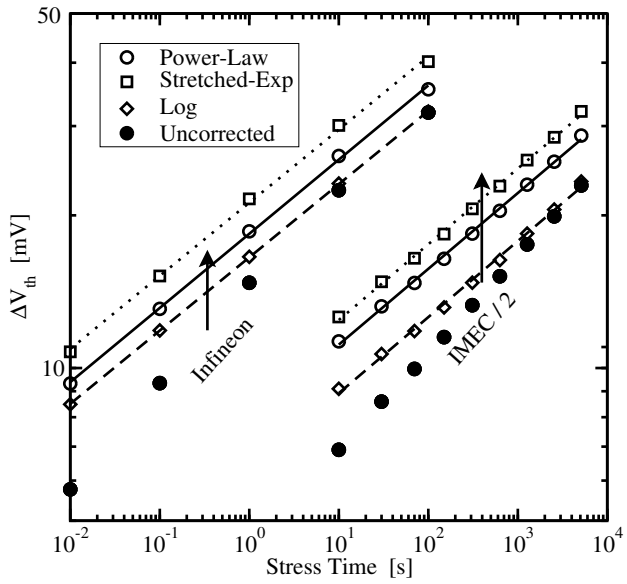

Fig. 6: Corrected results using the three universal relaxation functions for the MSM data of Reisinger *et al.* [7] (Infineon) and Kaczer *et al.* [5] (IMEC). Independently of the relaxation function the same power-law exponent is obtained while the prefactor depends much stronger on the choice of r. For the sake of clarity, the IMEC data has been divided by a factor of 2.

	Infineon		IMEC	
Analytic Form	A [mV]	n	A [mV]	n
Uncorrected	14.1	0.1866	8.9	0.1918
Log	16.5	0.1444	12.6	0.1499
Power-Law	18.4	0.1462	15.8	0.1495
Stretched-Exp	21.2	0.1441	17.6	0.1493

TABLE I: Influence of the various analytical expressions on the corrected slope and prefactor for a fit expression of the form At^n. Although the prefactor depends on the correction method, the more important slope is virtually independent of it.

component $P(t_s)$, which would have to be subtracted according to (4) before studying universality [27].

To judge the implications of the uncertainty related to the floating behavior of the final universal curve, we use the universal relaxation relation (11) to extrapolate from each measurement point to its 'true' value. Interestingly, one observes that in this particular case all relaxation functions result in the **same power-law exponent** while only the prefactors depend significantly on the choice of $r(\xi)$. This is demonstrated in Fig. 6 for the relaxation data of Reisinger *et al.* [7] and Kaczer *et al.* [5]. Interestingly, although the uncorrected data of Reisinger *et al.* have quite a visible curvature on a log-log plot and are as such not well described by a power-law, the corrected version can be very well described by a power-law with exponent $n = 0.15$. We recall that a deviation of the initial data from a power-law was one of the reasons why Reisinger *et al.* concluded that a log-like hole-trapping component has to be superimposed to a standard H-RD power-law with exponent $n = 1/4$. We thus conclude that even ultrafast measurements with $t_M = 1\,\mu$s **are not fast enough for obtaining the 'true' slope**, at least not for $t_s < 100$s. This can also be directly observed in Fig. 3 where only the data obtained for $t_s = 100$s shows signs of saturation.

The delayed and corrected values for the exponent and the prefactor are summarized in Table I, which confirms that the differences in

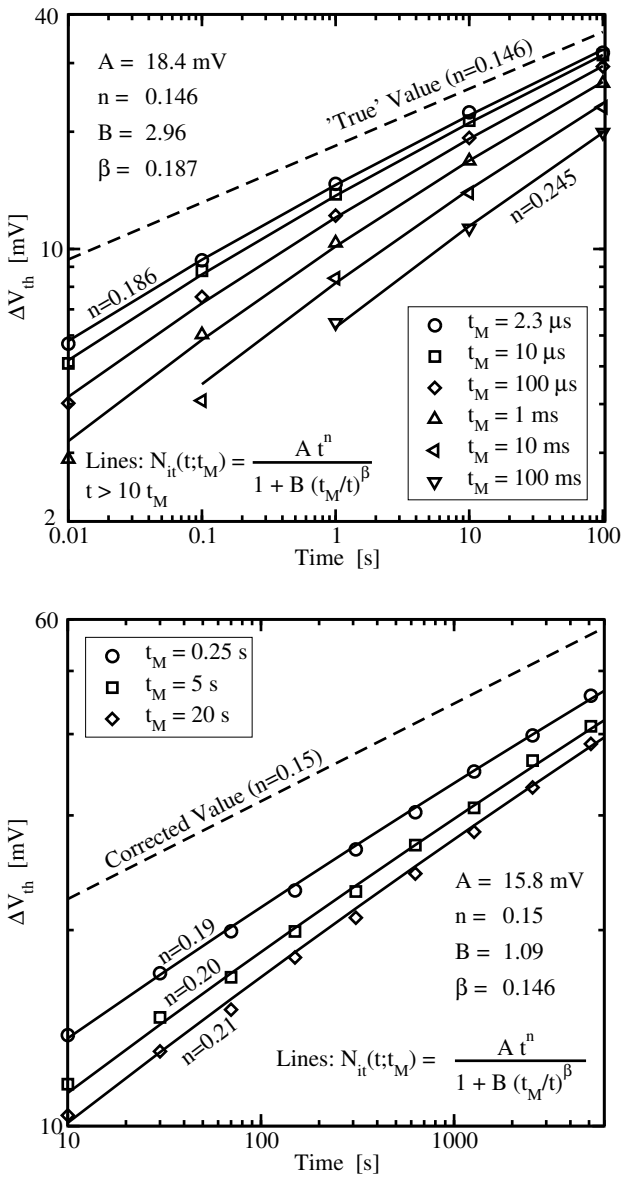

Fig. 7: Comparison of the analytic model for MSM measurements based on the universal relaxation to the data of Reisinger *et al.* [7] (top) and Kaczer *et al.* [5] (bottom). Excellent accuracy of the analytic model is obtained for all available delay times. In addition, the 'true' NBTI degradation can be recovered by extrapolating to $t_M = 0$s.

the values for the corrected exponents are well below the measurement accuracy. Thus, even if the empirical relaxation functions given by (7) – (9) contain some uncertainty, the influence on the corrected power-law exponent is probably small and the correct exponent can be expected to reflect the true degradation in a much better way than the uncorrected result. Also, the corrected exponents agree very well with exponents reported in some recent publications obtained from OTF measurements [9, 23].

B. Influence of Measurement-Delay on the Power-Law Parameters

Next, we show that the universal relaxation expression naturally connects individual stress curves obtained using the MSM technique with different delay times. For simplicity we assume that the true

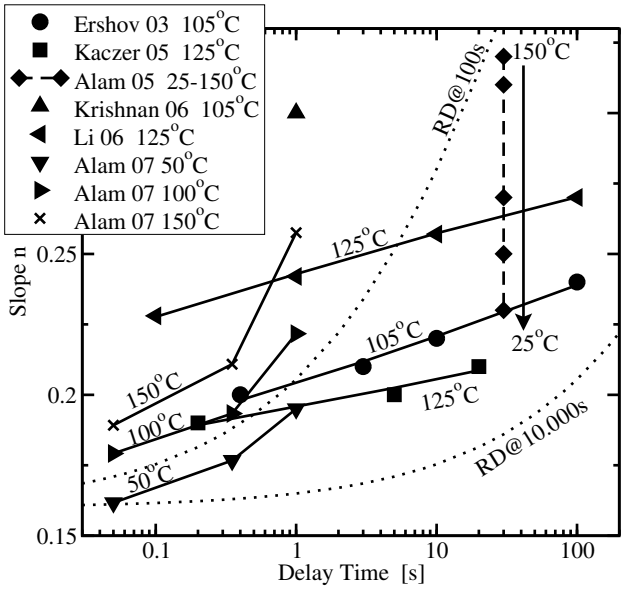

Fig. 8: Influence of the measurement delay on the measured slope as reported by various groups. The solid lines are given by a fit to (14) using the parameters in Table II. Note the strong temperature-dependence of the reported slopes and that the slopes were found to be constant over 3-4 decades in many measurements. Clearly, there is a large spread in the measurement data indicating a technology dependence. The dotted lines show the slopes predicted by the RD model at $t_s = 100\,\mathrm{s}$ and $t_s = 10,000\,\mathrm{s}$. Note that the RD slope changes considerably within two decades, is per construction temperature independent, and cannot be adjusted to the technology.

Source	T	n	B	β
Ershov [21]	105	0.15 (fixed)	1.49	0.179
Kaczer [5]	125	0.15 (fixed)	1.29	0.136
Li [33]	125	0.15 (fixed)	4.08	0.163
Alam [17]	50	0.155	4.79	0.611
Alam [17]	100	0.177	40.23	0.973
Alam [17]	150	0.186	102.2	1.048

TABLE II: The parameters for (14) used to fit the data in Fig. 8 assuming $t_s = 1,000\,\mathrm{s}$. The fit was obtained using a fixed $n = 0.15$ with a simple least-square algorithm. However, in order to fit the data of [17], which are different from the other sources considered in this study, n had to be included as a free parameter. Keep in mind that these values should be taken with care, since they were extracted by a fit to three or four rather inaccurate slope values using two/three free parameters. The inaccuracy of the slope values is a result of both the measurement uncertainty as well as the time-dependence of the slope.

degradation behavior follows a power-law as $S(t_s) = At_s^n$ and that the universal relaxation is given by (7). Due to the measurement delay one observes instead of the power-law

$$S_M(t_s,t_M) = S(t_s)\,r(t_s,t_M) = \frac{At_s^n}{1+B(t_M/t_s)^\beta}\ . \qquad (13)$$

Equation (13) is validated against the Infineon and IMEC data in Fig. 7 where the parameters B and β are given by the universal relaxation law. The analytic expression (13) exactly reproduces the delayed measurement results for various delay times t_M and thereby convincingly confirms our assumptions stated above.

As a consequence of the measurement delay, the *observed* power-law exponent n_M will be time-dependent and given through (13) as

$$n_M(t_s,t_M) = n - r'(t_M/t_s)\frac{t_M/t_s}{r} = n + \frac{\beta B}{B+(t_s/t_M)^\beta} \qquad (14)$$

with $r'(\xi) = \partial r(\xi)/\partial\xi$. It is worthwhile to stress that although many groups report a 'constant' measured power-law exponent over 3-4 decades which varies as a function of the temperature and delay-time, this can of course only be approximately correct. The fact that all curves obtained with different delay-times have to merge at larger times, makes a time-dependent slope a necessity. However, depending on the actual values of B and β this time-dependence will be more-or-less visible in a log-log plot. In general, the smaller β, the less visible the time-dependence will be. A comparison of measured power-law exponents as a function of the delay time t_M and temperature is given in Fig. 8. Most of the data shows an apparently constant power-law exponent (within the measurement accuracy) over 3-4 decades. Clearly, the measured power-law exponents, and consequently B and/or β (see Table II), depend on temperature and on the particular technology.

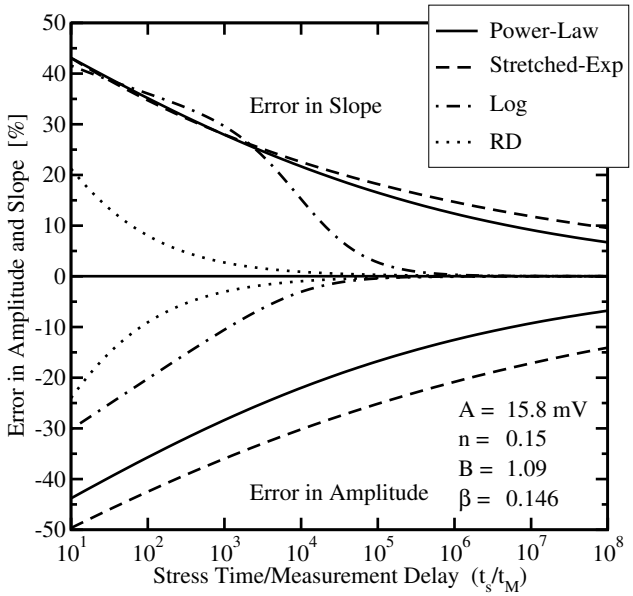

Fig. 9: Error in the slope (top) and prefactor (bottom) introduced by the measurement delay for the IMEC data of Fig. 4 as a function of t_s/t_M. Based on the power-law correction and extrapolation one obtains that for the slope and prefactor to be accurate be within 10%, the stress time has to be at least six orders of magnitude larger than the measurement delay. Also shown is the prediction of the RD model which reaches the 10% criterion after $t_s = 10 \times t_M$, in contradiction to measurements.

The measurement delay related error in the slope and prefactor of a supposed power-law degradation can be studied analytically using (13). This is shown in Fig. 9 where these errors are displayed as a function of t_s/t_M using the parameters extracted from the IMEC data of Fig. 4. Naturally, all models confirm that as a consequence of the delay the slope is always overestimated while the prefactor is always underestimated. Of particular interest here is the different prediction of the three universal relaxation expressions. The power-law and the stretched-exponential predict that in order to obtain the slope and prefactor with an accuracy of 10%, the stress time t_s has to be at least six orders of magnitude larger than the measurement delay t_M. For example, to keep the stress time below $10^4\,\mathrm{s}$ requires a measurement delay smaller than 10 ms. In contrast, the logarithmic